Gain mechanism of femtosecond two-photon-excited lasing effect in atomic hydrogen

Ding, Pengji; Ruchkina, Maria; Liu, Yi; Alden, Marcus; Bood, Joakim

Published in:
Optics Letters

DOI:
10.1364/OL.44.002374

2019

Document Version:
Peer reviewed version (aka post-print)

Gain mechanism of femtosecond two-photon excited lasing effect in atomic hydrogen

Pengji Ding[1,*], Maria Ruchkina[1], Yi Liu[2], Marcus Aldén[1], and Joakim Bood[1]

1. Division of Combustion Physics, Department of Physics, Lund University, Box 118, Lund, Sweden
2. Shanghai Key Laboratory of Modern Optical System, University of Shanghai for Science and Technology, 516, Jungong Road, 200093 Shanghai, China

*Corresponding author: pengji.ding@forbrf.lth.se

Abstract

By aiming to establish single-ended standoff combustion diagnostics, bidirectional lasing emissions of atomic hydrogen at 656 nm wavelength have been generated via two-photon resonant excitation by focusing 205 nm femtosecond laser pulses into a premixed CH_4/O_2 flame. The forward lasing strength is approximately one order of magnitude stronger than that of the backward one, due to the geometry of traveling wave excitation over a 2-mm-long pencil-shaped gain volume and the short gain lifetime of 3.5 ps. The gain coefficient of hydrogen lasing was determined to approximate 52/cm. As for the underlying physics of hydrogen lasing, amplified spontaneous emission (ASE) occurs simultaneously with four-wave mixing (FWM), and ASE dominates in the forward direction, whereas the backward lasing is virtually only ASE.

"Air lasing effect," which refers to the generation of laser-like coherent emission in ambient atmosphere or with the main components of air, has attracted intense research activities in recent years (refer to [1] and references therein). Backwardpropagating air lasing is of particular interest because it could potentially revolutionize the field of atmospheric remote sensing. Due to their coherent nature, much stronger radiation strength compared to backscattered light, directionality, and small divergence, techniques based on backward lasing have potential to significantly improve the detection sensitivity. As far as we know, backward lasing is mainly achieved through two approaches: (1) multi-photon resonant excitation [2–9], and (2) non-resonant excitation via electron-molecule inelastic collisions in femtosecond laser filamentation [10-14]. In the first scenario, the backward lasing effect has been observed in various alkali vapors [15,16] and several atomic radicals and stable molecules, such as O, H, C, N, CO, and NH_3 [2,4-6] using nanosecond/picosecond 2- or 3-photon excitation in various flames, where these species are naturally present. In ambient air, backward lasing in O, N, H, Ar atoms and water molecules has recently been generated via multiphoton resonant excitation as well [1,5]. For N and O lasing, the signal strength can be significantly enhanced through pre-dissociation of N_2 and O_2 using an additional preceding laser pulse of higher pulse energy [6].

Interestingly, with nanosecond laser pumping it has been frequently observed that the signal strength of backward lasing is comparable with [2,4], or in a few reported experiments [6,8] even stronger than the intensity of the forward lasing. Furthermore, the forward lasing signal is negatively correlated with the backward one, i.e., they compete with each other [6]. Recently, lasing of atomic oxygen in air through femtosecond two-photon pumping was reported [17], and it was observed that the backward 845-nm lasing signal was about an order of magnitude stronger than the forward lasing signal. The physical mechanism behind these observations has not yet been fully revealed. There are four candidate mechanisms that could be responsible for

the generation of the lasing effect: (1) amplified spontaneous emission (ASE), which should be equally effective in both forward and backward direction; (2) hyper-Raman gain, which also should be equally effective in both directions; (3) four-wave mixing (FWM), which should only give rise to emission in the forward direction due to phase-matching considerations; and (4) coherence-brightened superfluorescence (SF). Thus, all of these mechanisms might influence the lasing process and their relative importance is likely dependent on the prevailing experimental conditions. In order to develop optimum remote sensing and stand-off detection techniques, it is crucial to understand the underlying physics in order to enhance the backward lasing signal or control the ratio between the forward and backward lasing signals.

Recently, our group observed bidirectional 656 nm lasing from hydrogen atoms via 2-photon deep-UV excitation in a flame by using femtosecond 205 nm laser pulses [18,19]. As shown in Fig. 1(a), the 2-photon excitation is from the $(1s)^2S$ ground state to the $(3s)^2S$ (or $(3d)^2D$) excited state, and 656 nm (Balmer-α) photons are emitted when the H atom relaxes to the $(2s)^2S$ (or $(2p)^2P$) state. In a CH_4/O_2 flame, hydrogen atoms are naturally present, and therefore such a flame is a suitable medium to study the underlying physics of femtosecond laser-pumped atomic lasing. Unlike air lasing based on oxygen or nitrogen atoms, photodissociation of a parent molecule is not needed in this case. In contrast to the observation reported in [17], in the present work we have observed that the forward 656 nm lasing intensity is about one order of magnitude stronger than the backward lasing intensity and that the two lasing signals are positively correlated. Spectroscopic studies of lasing pulses in both directions reveal that the forward lasing pulse has a much broader linewidth compared to that of backward lasing pulse, suggesting that FWM occurs together with ASE in forward direction. On the other hand, the linewidth of the backward lasing pulse remains constant with varying pump laser wavelength, indicating that only ASE is responsible for the generation of the backward signal.

In the experiments, we used a 10 Hz-repetition-rate femtosecond laser system, which provided 205 nm laser pulses with a duration of ~125 fs (FWHM) and a maximum pulse energy of ~60 μJ. The laser beam diameter was about 5 mm. A schematic illustration of the experimental setup is shown in Fig. 1. First, the 205 nm laser beam propagated through a bulk CaF_2 equilateral dispersive prism not only to discriminate against radiation at other wavelengths from the femtosecond laser system, but also to spatially separate the backward-propagating 656 nm lasing emission. After the prism, the 205 nm laser pulse, with a maximum energy of ~25 μJ, was focused by a spherical lens (f = 30 cm) into a stoichiometric CH_4/O_2 flame, burning on a welding torch. The nozzle diameter of the welding torch is 1.5 mm. The size of the 205 nm beam at the focus was measured to ~600 μm horizontally and ~100 μm vertically.

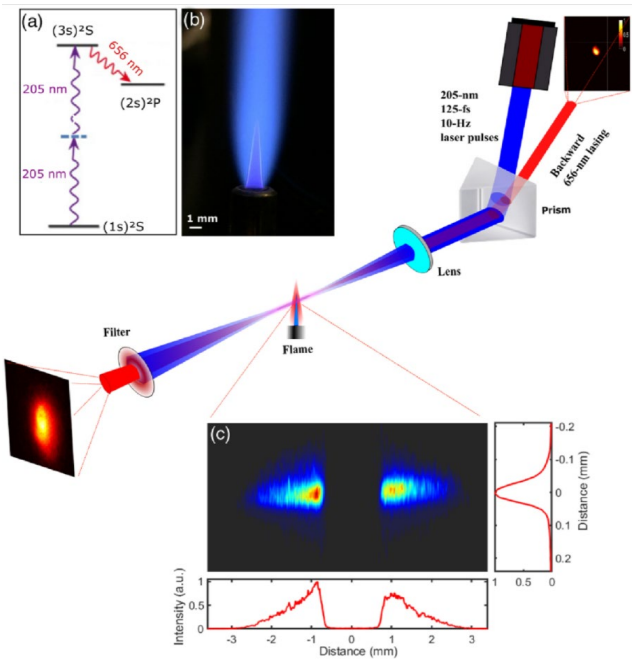

Fig. 1 *Schematic illustration of the experimental setup for generating bidirectional 656 nm hydrogen lasing with 205 nm femtosecond laser pulses in a premixed CH_4/O_2 flame. The spatial profiles of both the forward and backward lasing beams, recorded with a CCD camera, are also shown. The insets are: (a) energy level diagram relevant to the hydrogen lasing; (b) flame-brightness image of the CH_4/O_2 welding torch flame: (c) laser-induced fluorescence (LIF) image captured with an iCCD camera in side direction, where the solid line shows the profiles of spatial distribution of H atoms. A similar result has been shown in [18].*

Lasing pulses of 656 nm wavelength were generated in both the forward and backward directions. A spectrometer (Princeton Instruments, Acton SP2500, spectral resolution ~0.018

nm) was used to measure the spectra, and a charge-coupled device (CCD) camera (Optronis, ANIMA-PX 19.8 mm × 14.4 mm, resolution 1392 × 1024 pixels) was used to simultaneously monitor both lasing pulses. In the side direction, an intensified CCD camera (PI-MAX IV, Princeton Instruments) equipped with a f = 50 mm camera lens (f# = 1.2, Nikon) was employed to measure the spatial distribution of hydrogen atoms by capturing the laser-induced fluorescence emitted at 656 nm, which reflects the excitation volume, as shown in Fig. 1(c).

First, the spectra of both the forward and backward 656 nm lasing pulses were measured with the pump laser tuned to the optimal excitation wavelength at 205.15 nm, as shown in Fig. 2(a). It is clear that the spectrum of the forward lasing pulse is significantly broader than that of the backward lasing pulse. The spectral width (FWHM) of the forward lasing signal is approximately 0.32 nm, while it is about 0.14 nm for the backward lasing signal. This feature suggests that FWM occurs in the forward direction because it produces a broader spectrum due to the virtual intermediate state involved. In this case, the FWM process involves two 205 nm photons, one 656 nm photon, and another photon around 121.5 nm corresponding to the $2s^2P \rightarrow 1s^2S$ transition. Note that similar features have been observed in experiments with argon lasing at 1409 nm wavelength generated through femtosecond 3-photon excitation, where a six-wave mixing process is found to dominate in the forward direction [20,21].

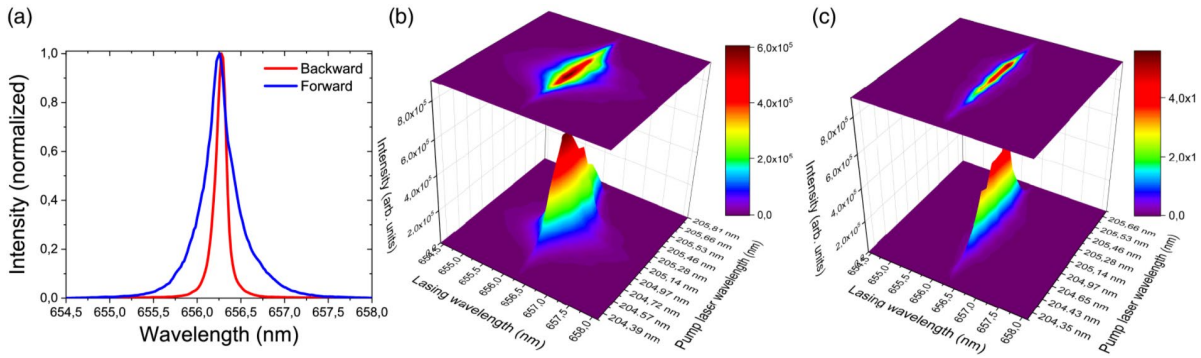

Fig. 2 *(a) Comparison between the spectra of forward and backward lasing pulses pumped by resonant 205.15 nm laser pulse; (b)–(c) the spectra of forward and backward lasing pulses for different pump laser wavelengths ranging from 204.69 to 205.81 nm. For every pump laser wavelength, the spectrum was integrated over 10 shots. The slit width of PI spectrometer is 25 μm, and the pump pulse energy is about 14 μJ.*

To shed more light on the FWM process, the spectra of both forward and backward 656 nm lasing signals were systematically recorded for different pump laser wavelengths ranging from 204.69 to 205.82 nm. The results for forward and backward lasing are shown in Figs. 2(b) and 2(c), respectively. For the forward lasing spectrum, the spectral width increases with decreasing detuning of the pump laser from the resonance. This characteristic is different from the behavior of the spectral width of the backward lasing pulse, which basically remains the same for different pump laser wavelengths. Note that for both forward and backward lasing spectra, their central wavelengths are identical within the experimental uncertainty. These results unambiguously indicate that a resonance-enhanced FWM process contributes to the forward lasing, simultaneously evolving with ASE, whereas the backward lasing is virtually only ASE.

During the experiments, we noticed that the forward lasing beam appeared to be much stronger than the backward one. Therefore, simultaneous measurements of both the forward and backward 656 nm lasing pulses were conducted using a CCD camera. The spatial profiles are shown in Fig. 3. Apparently, the forward lasing signal is more divergent than the backward lasing signal. A rough estimation of the divergence of the forward lasing beam is around 100 mrad, while that of the backward lasing beam is approximately 20 mrad, which is consistent with our previous result [19]. We integrated the overall signals for both the forward and backward lasing, and plotted the integrated signal of forward lasing as a function of that of backward lasing, as shown in Fig. 3. A linear fit to the data suggests a slope of ~10. This result indicates that, on the one hand, forward lasing is positively correlated with backward lasing, yet, on the other hand, forward lasing strength, on average, is about one order of magnitude stronger than the backward lasing strength. These observations are different from what have been reported previously in similar two-photon excited lasing schemes [4,6,8,17], where the lasing intensity in the forward direction is reported to be approximately equal to, or weaker than, that in the backward direction.

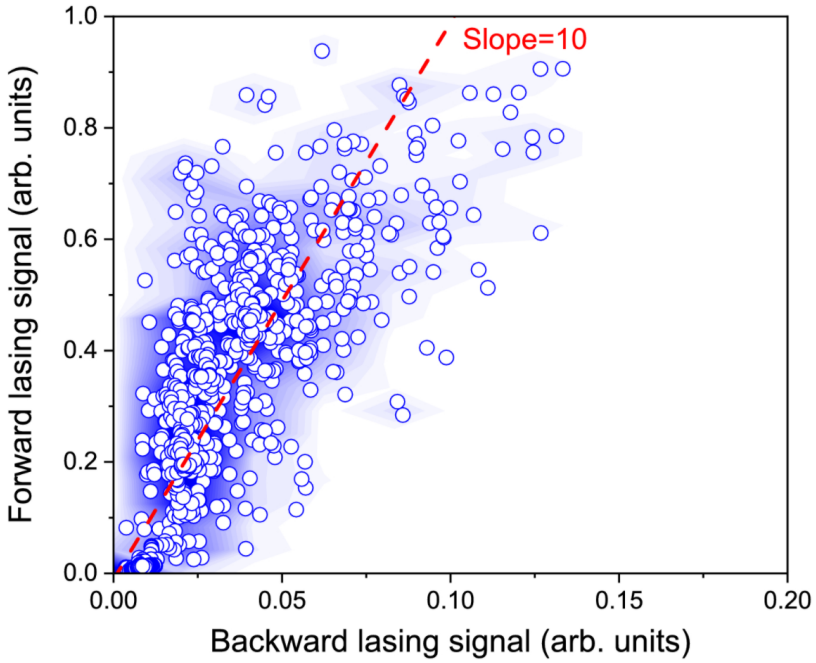

Fig. 3 *Density plot of the correlation between the forward and backward 656 nm lasing signals (normalized), where the blue dots represent data recorded for 660 shots. The red dashed line represents linear fitting to the data.*

Similar experimental observations, i.e., that forward lasing is more divergent and much stronger than the backward lasing, were also observed in 337-nm lasing in neutral nitrogen molecules [14]. In that case, the pumping process was enabled via electron-molecule inelastic collisions in a femtosecond laser filament, which is not a resonant pumping process. It was observed that the forward 337-nm lasing strength was about 3 orders of magnitude stronger than the backward one. This dramatic asymmetry of lasing intensities in the two directions was attributed to the nature of the traveling wave excitation in the pumping process, given that the effective gain lifetime (~15 ps) is much shorter than the propagation time over a ~3-cm-long excitation volume.

In the current experiments with two-photon resonant pumping, the longitudinal length of the roughly cylindrically shaped excitation volume was approximately 2 mm, which is about 20 times larger than its transverse diameter. Thus, the gain medium can be regarded as pencil-shaped, and therefore the traveling-wave excitation contributes by generating stronger 656 nm lasing in the forward than in the backward direction. In the forward direction, the lasing signal

is continuously amplified following the wake of the gain wave induced by the femtosecond pump pulse with a small delay throughout the whole excitation volume. On the contrary, the initial backward lasing signal starts from the end of the excitation volume and experiences decaying gain on the way back through the excitation volume. This results in a much weaker and delayed backward lasing pulse compared to the forward one.

Thus, it is essential to explore the gain dynamics of the hydrogen lasing, which we have done by injecting a weak femtosecond seeding pulse, centered at 656 nm, into the gain medium, together with the 205 nm pump pulse. The 656 nm seeding pulses were provided by another similar OPA unit. The diameter of the seeding beam inside the jet flame was about 1 mm, approximately 10 times larger than the size of the excitation volume created by the 12 μJ 205 nm pump pulse. The crossing angle between the 205 nm pump beam and the 656 nm seeding beam was 1.1 deg. In the far field, the 205 nm pump beam was terminated in a beam dump, and an interference filter (transmission maximum at 656 nm and bandpass width ~15 nm FWHM) was used to suppress radiation at other wavelengths than that of the seeding beam and the induced lasing. A fiber-based spectrometer (FLAME-S-UV-VIS Spectrometer, Ocean Optics) was used to probe the 656 nm signal. As shown in Fig. 4(a), the weak 656 nm signal increased significantly when the pump pulse and the seeding pulse are spatiotemporally overlapped; ~30 times stronger than the seed intensity. By considering the following facts: (1) the seeding beam diameter is ~10 times larger than the cross section of the excitation volume; and (2) the 2 nm spectral bandwidth of the seeding pulse is about twice broader than the absorption linewidth of the $(2s)^2S \rightarrow (3s)^2S/(3d)^2D$ transition, we can estimate the effective amplification of the seeding pulse to be 3×10^4. The longitudinal length of the excitation volume was determined by measuring the 656 nm fluorescence profile from the side, and it was found to be ~2 mm. Based on this length, we estimated the optical gain coefficient from $e\alpha L = 3 \times 10^4$, which results in $\alpha \approx 52$ cm^{-1}. This gain coefficient is comparable to those

reported previously for similar two-photon-excited lasing, for instance $\alpha \approx 62$ cm^{-1} for atomic oxygen and $\alpha \approx 71$ cm^{-1} for nitrogen [5,6]. It should be noted that the real gain coefficient should be larger than 52 cm^{-1} if the spatial overlap between pump and seed laser beams were perfectly collinear.

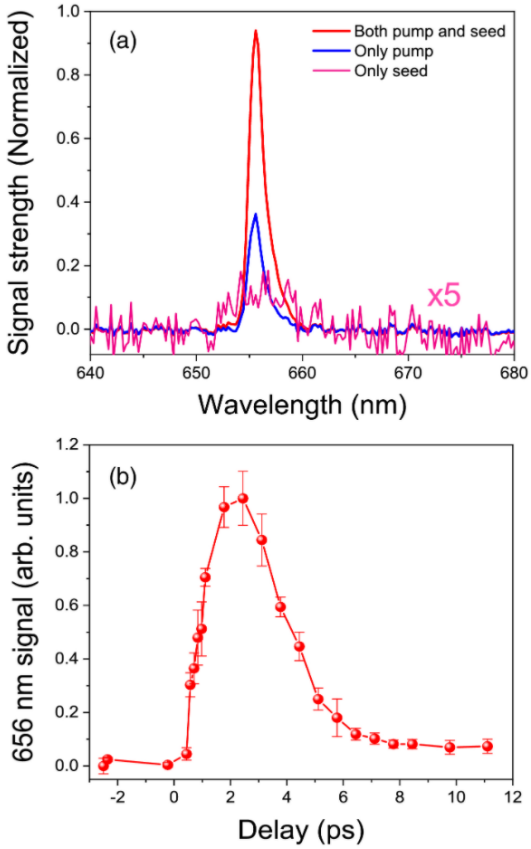

Fig. 4 *(a) Amplification of the 656 nm lasing signal by injecting a weak seeding pulse. Note that the seed signal itself is magnified 5 times for clarity. (b) Gain dynamics measurement, i.e., the amplified 656 nm signal as a function of the delay between the 205 nm pump pulse and the 656 nm seeding pulse. Negative delay corresponds to a situation where the seeding pulse is ahead of the pump pulse.*

By varying the temporal delay between the 205 nm pump laser pulse and the 656 nm seeding pulse, the gain dynamics was studied, and the result is shown in Fig. 4(b). A maximum occurs ~2 ps after the amplification starts. The gain is observed to last for ~3.5 ps (FWHM), which is shorter than the traveling time of the pump laser pulse over 2-mm-long excitation volume. This again confirms our speculation that the energy asymmetry of the forward and backward lasing is mainly due to the traveling excitation. It has already been mentioned that both FWM and ASE processes contribute to the forward 656 nm lasing; however, there is no information

about which process dominates. The present study of the gain dynamics suggests that ASE dominates over FWM, because if not, one would expect the measured gain lifetime to be in the order of the temporal duration of the pump pulse, i.e., 125 fs.

In conclusion, we experimentally studied bidirectional 656 nm lasing of atomic hydrogen in a methane/oxygen flame pumped with 205 nm femtosecond laser pulses. A substantial asymmetry between the lasing intensities in the forward and backward directions was observed, where the forward lasing signal was found to be about one order of magnitude stronger than backward lasing intensity. The reason for this is attributed to the nature of traveling-wave excitation in our experiment and a finite gain lifetime of 3.5 ps. The gain coefficient was measured and found to be about 52 cm^{-1}. Measurements of spectral properties and gain dynamics of the 656 nm lasing suggest that both FWM and ASE processes contribute to the forward lasing emission and that the ASE process dominates over the FWM. By contrary, the backward lasing emission is virtually only ASE.

Funding

Knut och Alice Wallenbergs Stiftelse via the Centre for Combustion Science and Technology (22538-4); H2020 European Research Council (ERC) (TUCLA).

References

1. P. Polynkin and Y. Cheng, Air Lasing (Springer International Publishing, 2018), Vol. 208.
2. M. Aldén, U. Westblom, and J. E. M. Goldsmith, Opt. Lett. 14, 305 (1989).
3. J. E. M. Goldsmith, J. Opt. Soc. Am. B 6, 1979 (1989).
4. U. Westblom, S. Agrup, M. Aldén, H. M. Hertz, and J. E. M. Goldsmith, Appl. Phys. B 50, 487 (1990).
5. A. Dogariu, J. B. Michael, M. O. Scully, and R. B. Miles, Science 331, 442 (2011).

6. A. Laurain, M. Scheller, and P. Polynkin, Phys. Rev. Lett. 113, 253901 (2014).
7. P. R. Hemmer, R. B. Miles, P. Polynkin, T. Siebert, A. V. Sokolov, P. Sprangle, and M. O. Scully, Proc. Natl. Acad. Sci. USA 108, 3130 (2011).
8. A. J. Traverso, R. Sanchez-Gonzalez, L. Yuan, K. Wang, D. V. Voronine, A. M. Zheltikov, Y. Rostovtsev, V. A. Sautenkov, A. V. Sokolov, S. W. North, and M. O. Scully, Proc. Natl. Acad. Sci. USA 109, 15185 (2012).
9. A. M. Akulshin, F. P. Bustos, and D. Budker, Opt. Lett. 43, 5279 (2018).
10. P. Sprangle, J. Peñano, B. Hafizi, D. Gordon, and M. Scully, Appl. Phys. Lett. 98, 211102 (2011).
11. S. Mitryukovskiy, Y. Liu, P. Ding, A. Houard, and A. Mysyrowicz, Opt. Express 22, 12750 (2014).
12. P. Ding, S. Mitryukovskiy, A. Houard, E. Oliva, A. Couairon, A. Mysyrowicz, and Y. Liu, Opt. Express 22, 29964 (2014).
13. P. Ding, E. Oliva, A. Houard, A. Mysyrowicz, and Y. Liu, Phys. Rev. A 94, 043824 (2016).
14. P. Ding, "Lasing effect in femtosecond filaments in air," thesis (Université Paris-Saclay, 2016).
15. M. S. Malcuit, D. J. Gauthier, and R. W. Boyd, Phys. Rev. Lett. 55, 1086 (1985).
16. R. W. Boyd, M. S. Malcuit, D. J. Gauthier, and K. Rzązewski, Phys. Rev. A 35, 1648 (1987).
17. S. Alisauskas, A. Baltuska, R. Boyd, and P. Polynkin, in European Conference on Lasers and Electro-Optics—European Quantum Electronics Conference (Optical Society of America, 2015), pp. PD-A-4.
18. M. Ruchkina, P. Ding, A. Ehn, M. Aldén, and J. Bood, Proc. Combust. Inst. 37, 1281 (2019).
19. P. Ding, M. Ruchkina, Y. Liu, M. Alden, and J. Bood, Opt. Lett. 43, 1183 (2018).

20. A. Dogariu and R. B. Miles, in Conference on Lasers and ElectroOptics (Optical Society of America, 2018), p. JTh5B.8.
21. A. Dogariu and R. B. Miles, Opt. Express 24, A544 (2016).